International Journal of Solids and Structures 47 (2010) 2056–2061

Contents lists available at ScienceDirect

International Journal of Solids and Structures

journal homepage: www.elsevier.com/locate/ijsolstr

On non-physical response in models for fiber-reinforced hyperelastic materials

J. Helfenstein [a,*], M. Jabareen [a,b], E. Mazza [a,c], S. Govindjee [a,d]

[a] Department of Mechanical and Process Engineering, Swiss Federal Institute of Technology Zurich, Tannenstrasse 3, 8092 Zurich, Switzerland
[b] Faculty of Civil and Environmental Engineering, Technion, Israel Institute of Technology, Haifa 32000, Israel
[c] EMPA, Swiss Federal Laboratories for Materials Testing and Research, Überlandstrasse 129, 8600 Dübendorf, Switzerland
[d] Department of Civil Engineering, University of California, 709 Davis Hall, Berkeley, CA 94720-1710, USA

ARTICLE INFO

Article history:
Received 16 December 2009
Received in revised form 31 March 2010
Available online 13 April 2010

Keywords:
Hyperelasticity
Anisotropy
Fiber-reinforced
Quasi-incompressible
Volume growth

ABSTRACT

Soft biological tissues are sometimes composed of thin and stiff collagen fibers in a soft matrix leading to a strong anisotropy. Commonly, constitutive models for quasi-incompressible materials, as for soft biological tissues, make use of an additive split of the Helmholz free-energy into a volumetric and a deviatoric part that is applied to the matrix and fiber contribution. This split offers conceptual and numerical advantages. The purpose of this paper is to investigate a non-physical effect that arises thereof. In fact, simulations involving uniaxial stress configurations reveal volume growth at rather small stretches. Numerical methods such as the Augmented Lagrangian method might be used to suppress this behavior. An alternative approach, proposed here, solves this problem on the constitutive level.

1. Introduction

Soft matter often exhibits complex mechanical behavior related to inhomogeneity, anisotropy and (near) incompressibility. This is the case for soft biological tissues that are sometimes characterized by strong anisotropy due to the presence of thin and stiff collagen fibers in a soft extracellular matrix. Examples for this are ligaments and tendons, arterial walls or the annulus fibrosus. Under physiological conditions these tissues might undergo large deformations, necessitating a mechanical description in the framework of nonlinear continuum mechanics. Numerical methods are often used to simulate and understand their mechanical behavior. This has motivated a number of recent studies on constitutive modeling approaches for fiber-reinforced hyperelastic materials.

Classical hyperelastic models, such as the polynomial forms (Rivlin and Saunders, 1951) or the Ogden model (Ogden, 1972) were designed for the modeling of isotropic materials. Later, these models were modified to allow for an additive split of the Helmholz free-energy into a volumetric and a deviatoric part, to some extent motivated by the multiplicative decomposition of the deformation gradient introduced by Flory (1961). It was shown by Ehlers and Eipper (1998) that, if this split is applied to materials not restricted to (nearly) incompressible behavior, it might lead to unphysical responses in uniaxial tension.

Anisotropy itself can be modeled by explicitly including a fiber contribution in the strain energy formulation. Thereby, the idea of the additive split might also be applied to the fiber contribution. To our best knowledge, the first fiber-reinforced model using this additive split assumption for (nearly) incompressible materials was proposed by Weiss et al. (1996). In 2000, Holzapfel et al. published a model that has since then become very popular in simulations involving anisotropic biological tissues.

The purpose of this paper is to investigate a non-physical effect in the application of the additive split to fiber-reinforced (nearly) incompressible materials. In fact, numerical simulations involving uniaxial stress configurations lead to volume growth when using the models by Weiss et al. (1996) or Holzapfel et al. (2000). To prevent this behavior, numerical costly methods such as the Augmented Lagrangian method (Simo and Taylor, 1991) might be used.

An alternative approach, as proposed here, is to avoid the multiplicative decomposition of the deformation gradient in the fiber contribution. Although several authors (Holzapfel et al., 2004; Schröder et al., 2005) have already proposed model formulations without this decomposition, no statements were found in the papers that this was motivated by the problems reported in the present work. In general, no criterion is proposed for or against this decomposition being applied to the fiber contributions to the free-energy. Rather it seems the invariants and their modified equivalents are considered "to be equivalent" in case of incompressibility. Though it will be shown in this paper that the choice of either one has an influence on the stress and stiffness terms of the fiber contribution.

Our results are also compared with the predictions from the model proposed by Rubin and Bodner (2002), which avoids the

* Corresponding author. Tel.: +41 (0) 44 632 2886; fax: +41 (0) 44 632 1145.
E-mail addresses: joerg.helfenstein@imes.mavt.ethz.ch (J. Helfenstein), cvjmah@technion.ac.il (M. Jabareen), edoardo.mazza@imes.mavt.ethz.ch (E. Mazza), sanjay@ce.berkeley.edu (S. Govindjee).

0020-7683/$ - see front matter © 2010 Elsevier Ltd. All rights reserved.
doi:10.1016/j.ijsolstr.2010.04.005

volumetric split for the fiber contribution and uses an additive split in the log-energies.

2. Methods

2.1. Continuum mechanics background

For Green elastic materials the Cauchy (true) stress $\boldsymbol{\sigma}$ and the spatial stiffness $\mathbb{c}$ can be obtained from a strain energy density function Ψ (the Helmholz free-energy per unit reference volume) by

$$\boldsymbol{\sigma} = \frac{2}{J}\boldsymbol{\chi}_*\left[\frac{\partial \Psi[\mathbf{C}]}{\partial \mathbf{C}}\right], \quad \mathbb{c} = \frac{4}{J}\boldsymbol{\chi}_*\left[\frac{\partial^2 \Psi[\mathbf{C}]}{\partial \mathbf{C}\partial \mathbf{C}}\right], \tag{1}$$

respectively.[1] Here, $\boldsymbol{\chi}^*[]$ is the push-forward operator to bring the material derivatives to the spatial configuration. Ψ depends solely on the right Cauchy–Green deformation tensor $\mathbf{C} = \mathbf{F}^{\mathrm{T}}\mathbf{F}$, where $\mathbf{F}$ is the deformation gradient and $()^{\mathrm{T}}$ depicts the usual transpose of a second order tensor.

Anisotropy due to fibers can be included by use of structural tensors

$$\mathbf{A}^{(i)} = \boldsymbol{\zeta}^{(i)} \otimes \boldsymbol{\zeta}^{(i)}, \tag{2}$$

where $\boldsymbol{\zeta}^{(i)}$ is a normalized vector describing the orientation of the ith fiber family in the reference configuration. The principles of material frame indifference and invariance under transformations that respect the material symmetries lead to a representation of Ψ that depends only on the so called mixed invariants of $\mathbf{C}$ and $\mathbf{A}^{(i)}$:

$$\Psi = \Psi[I_1,\ I_2,\ I_3,\ I_4^{(i)}] \tag{3}$$

with

$$I_1 = \mathrm{tr}[\mathbf{C}], \tag{4a}$$

$$I_2 = \frac{1}{2}\left((\mathrm{tr}[\mathbf{C}])^2 - \mathrm{tr}[\mathbf{C}^2]\right), \tag{4b}$$

$$I_3 = \det[\mathbf{C}] = J^2, \tag{4c}$$

$$I_4^{(i)} = \boldsymbol{\zeta}^{(i)} \cdot \mathbf{C}\boldsymbol{\zeta}^{(i)} = \mathbf{C} : \mathbf{A}^{(i)} = (\zeta^{(i)})^2. \tag{4d}$$

$J = \det[\mathbf{F}]$ denotes the volume ratio and $I_4^{(i)}$ represents the square of the stretch $\zeta^{(i)}$ of fiber family i. Note that the set of invariants I_γ, $\gamma = 1,\ldots,4$ is not the full set of invariants of the tensors $\mathbf{C}$ and $\mathbf{A}^{(i)}$ (Antman, 2005) but includes the commonly used ones.

The right Cauchy–Green tensor $\mathbf{C}$ can be split multiplicatively into a deviatoric part $\overline{\mathbf{C}}$ and a spherical part $\mathbf{C}_{\mathrm{vol}}$ (Flory, 1961):

$$\mathbf{C} = \mathbf{C}_{\mathrm{vol}}\overline{\mathbf{C}} = J^{2/3}\mathbf{I}\overline{\mathbf{C}}. \tag{5}$$

Using this split it is common to write the strain energy Ψ in an uncoupled form

$$\Psi = U[J] + \overline{\Psi}\left[\bar{I}_1,\ \bar{I}_2,\ \bar{I}_4^{(i)}\right] \tag{6}$$

in which U is the response of the material to volume changes and $\overline{\Psi}$ depends only on the distortional part of the deformation. $\bar{I}_1$, $\bar{I}_2$ and $\bar{I}_4^{(i)}$ are the invariants of the deviatoric part $\overline{\mathbf{C}}$ of the right Cauchy–Green deformation tensor $\mathbf{C}$. It should be noted that, in general, the invariant $\bar{I}_4^{(i)}$ no longer represents the square-stretch of fiber family i; rather,

$$\bar{I}_4^{(i)} = J^{-2/3}(\zeta^{(i)})^2. \tag{7}$$

The split (6) enables distinct modeling of high resistance to volumetric deformation and low resistance to distortional deformation (as in the case of nearly incompressible materials). Sansour (2008) shows that the additive split is a consequence of the assumption that the pressure is solely a function of J.

In case of fiber-reinforced materials $\overline{\Psi}$ can be divided into $\overline{\Psi}_{gs}$ and $\overline{\Psi}_f$ for the energy contributions of the matrix ("ground substance") and the fibers, respectively:

$$\Psi[\mathbf{C}, \mathbf{A}_i] = U[J] + \overline{\Psi}_{gs}[\bar{I}_1, \bar{I}_2] + \overline{\Psi}_f[\bar{I}_4^{(i)}]. \tag{8}$$

In the following, three structural, anisotropic constitutive models are presented. For ease of reading their notation has been unified from their original presentations. The closed forms of the stress and material stiffness tensors are given in the original papers.

2.1.1. Model proposed by Weiss et al. (1996)

Weiss et al. (1996) suggested a constitutive model that uses a strain energy function of the form (8). The individual contributions are given by

$$U[J] = \frac{\kappa}{2}(\ln[J])^2, \tag{9a}$$

$$\overline{\Psi}_{gs}[\bar{I}_1, \bar{I}_2] = w_1(\bar{I}_1 - 3) + w_2(\bar{I}_2 - 3), \tag{9b}$$

$$\overline{\Psi}_f[\bar{I}_4^{(i)}] = \frac{w_3}{w_4}\sum_{i=1}^{n}\left(\mathrm{e}^{w_4(\bar{I}_4^{(i)}-1)} - \bar{I}_4^{(i)w_4}\right) \tag{9c}$$

where κ is the small strain bulk modulus and the w_γ, $\gamma = 1,\ldots,4$, are material parameters. w_4 is introduced in the present work as an additional parameter that allows one to shift the onset of the fiber response and thus to fit the model to the selected uniaxial response ($w_4 = 1$ [−] retrieves the original model). Note that the contribution of the ground substance is described by a Mooney–Rivlin model (a special case of the polynomial materials Rivlin and Saunders, 1951) with the small strain shear modulus $\mu = 2(w_1 + w_2)$.

2.1.2. Model proposed by Holzapfel et al. (2000)

Holzapfel et al. (2000) proposed a model according to Eq. (8) for modeling the arterial wall. The explicit forms of the energy contributions are given by

$$U[J] = \frac{\kappa}{2}(J-1)^2, \tag{10a}$$

$$\overline{\Psi}_{gs}[\bar{I}_1] = \frac{\mu}{2}(\bar{I}_1 - 3), \tag{10b}$$

$$\overline{\Psi}_f[\bar{I}_4^{(i)}] = \frac{h_1}{2h_2}\sum_{i=1}^{n}\left(\mathrm{e}^{h_2(\bar{I}_4^{(i)}-1)^2} - 1\right), \tag{10c}$$

where κ, μ, h_1 and h_2 are the small strain bulk and shear moduli and two material parameters, respectively. The ground substance is modeled as a Neo-Hookean material.

In both these models the fibers are thought to be active only in tension and therefore all contributions (energy, stress and stiffness) of fiber family i are set to zero if $\bar{I}_4^{(i)} < 1$.

2.1.3. Model proposed by Rubin and Bodner (2002)

The model presented by Rubin and Bodner (2002) uses a different strain energy function:

$$\Psi = \frac{p}{2}\left(\exp^{p^{-1}\widehat{\Psi}} - 1\right), \tag{11}$$

where p is a material constant. $\widehat{\Psi}$ is the sum of four contributions

$$\widehat{\Psi} = \widehat{\Psi}_1[J] + \widehat{\Psi}_2[\bar{I}_1] + \widehat{\Psi}_3[\zeta_i] + \widehat{\Psi}_4[\alpha_1]. \tag{12}$$

The functions $\widehat{\Psi}_\gamma, \gamma = 1,\ldots,4$, characterize the response to total dilatation, total distortion, fiber stretching and distortional deformation of a dissipative component, respectively. $\widehat{\Psi}_4$ will be neglected here, reducing the model to pure elastic response:

[1] Our notation of tensor operators follows Holzapfel (2000).

$$\widehat{\Psi}_1[J] = 2\kappa((J-1) - \ln[J]), \tag{13a}$$

$$\widehat{\Psi}_2[\bar{I}_1] = \mu(\bar{I}_1 - 3), \tag{13b}$$

$$\widehat{\Psi}_3[\zeta_i] = \sum_{i=1}^{n} \frac{r_1}{r_2} \left\langle \zeta^{(i)} - 1 \right\rangle^{2r_2}, \tag{13c}$$

where μ and κ are the small strain shear and bulk moduli, respectively, r_1 and r_2 are material parameters and n is the number of fiber families. The McAuley bracket $\langle\cdot\rangle$ is defined by

$$\langle x \rangle = \frac{1}{2}(x + |x|) \tag{14}$$

and eliminates the energy contribution for $\zeta^{(i)} < 1$.

For the purpose of the present analysis, we also consider all three models where the measure of fiber stretch $\bar{I}_4$ is exchanged with the unmodified invariant I_4, for the first two models, and ζ with $\bar{\zeta}$ for the last model. Table 1 summarizes the different model formulations analyzed in this work.

All models can be shown to be polyconvex by following the procedures described in Schröder and Neff (2003), Hartmann and Neff (2003) and Balzani et al. (2006). The model by Weiss et al. (1996) is polyconvex only if $w_2 = 0$ [MPa] and the volume ratio J does not exceed the natural number e [−].

2.2. Numerical experiment

To investigate the behavior of the highlighted models, a simple example is selected that can easily be implemented numerically. It consists of a cube of homogeneous material that is aligned with a Cartesian coordinate system in three-dimensional space (cf. Fig. 1). One fiber family aligned with the 1-direction reinforces the material. The load consists of an uniaxial stress state in the fiber direction (the lateral surfaces of the cube are traction free).

The numerical experiment and all constitutive models were implemented in MATLAB (2005). Axial stretches are prescribed as boundary conditions, the lateral stretches are found by a numerical minimization of the strain energy using the MATLAB function *fminsearch*().

2.2.1. Calibration of the models

Even though we do not want to compare the predictive capabilities of the six models we do calibrate them for their responses to uniaxial tension in the fiber direction and in the transverse direction (where only the matrix is load bearing). This is done in order to activate the models similarly in the numerical experiment described above.

Numerical values for the parameters of model $\overline{H}$ are selected according to the results of an experimental program (Eberlein et al., 2001). All other models were calibrated to provide the same uniaxial response in the axial and transverse directions with respect to the fibers for stretches up to $\lambda_1 = 1.2$ [−].

The parameter set from Eberlein et al. (2001) is based on experimental data obtained for measurements with a stretch range from $\lambda_1 = 1$–1.08 [−]. Note that we extrapolated here the validity of these parameters for stretches up to 1.2 [−] but no experimental evidence exists of the practical relevance of such a model for $1.08 < \lambda_1 < 1.2$ [−].

Table 1
Models analyzed in this work and their references.

Reference	Name	Measure of fiber stretch
Weiss et al. (1996)	$\overline{W}$	$\bar{I}_4$
	W	I_4
Holzapfel et al. (2000)	$\overline{H}$	$\bar{I}_4$
	H	I_4
Rubin and Bodner (2002)	$\overline{R}$	$\bar{\zeta}_4$
	R	ζ_4

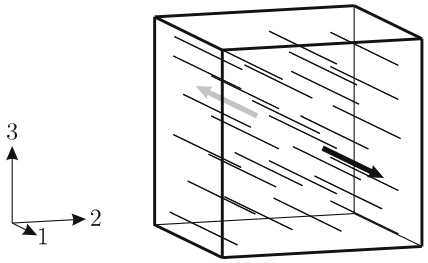

Fig. 1. Example configuration consisting of a cube that is reinforced with fibers in the one-direction and aligned with a Cartesian coordinate system. A stretch is applied in the fiber direction, whereas the lateral sides are traction free (uniaxial stress state).

For the calibration the small strain shear modulus is fixed for all models such that it equals the small strain shear modulus μ^* of the reference material. Furthermore, full incompressibility is assumed as it was done in the original parameter calibration (Eberlein et al., 2001) and therefore the parameters describing the volumetric response cannot be obtained by such a procedure. A reference small strain bulk modulus κ^* equal 2200 [MPa] is chosen, which corresponds to the bulk modulus of water (Rubin and Bodner, 2002) and is thus reasonably accurate for the materials of interest to us. The parameters describing the volumetric response of all models are chosen to give the same ratio of small strain bulk to shear modulus.

In order to guarantee the polyconvexity of the models W and $\overline{W}$ (if J does not exceed the natural number e [−]) the parameter w_2 was set equal 0.0 [MPa] a priori. Doing so, the models W, $\overline{W}$, H and $\overline{H}$ have the same ground substance contribution to the Helmholz free-energy and their response to uniaxial tension in the direction transverse to the fibers is the same.

As can be seen from Eqs. (11–13) the model proposed by Rubin and Bodner (2002) reduces in the limit case $p \to \infty$ [MPa] to a Neo-Hookean material similar to the models proposed by Weiss et al. (1996) (with $w_2 = 0$ [MPa]) and Holzapfel et al. (2000). In order to preserve the special structure of this model, we set $p = 1$ [MPa] and accept a non-perfect calibration of the models R and $\overline{R}$ in the direction transverse to the fibers.

Table 2 reports the parameters for all models that are used.

2.3. Instantaneous Poisson's ratio

The kinematic response of a fiber-reinforced cube under uniaxial tension in the fiber direction (cf. Section 2.2) is (normally) char-

Table 2
Material parameters of the models that were analyzed. The parameter set of model $\overline{H}$ was used as reference for the calibration of the other models.

	κ [MPa]	w_1 [MPa]	w_2 [MPa]	w_3 [MPa]	w_4 [−]
$\overline{W}$	κ^*	$\frac{1}{2}\mu^* - w_2$	0.000E+0	3.362E−4	3.864E+1
W	κ^*	$\frac{1}{2}\mu^* - w_2$	0.000E+0	6.689E−4	3.865E+1
	κ [MPa]	μ [MPa]	h_1 [MPa]	h_2 [−]	
$\overline{H}$	κ^*	μ^*	3.000E+0	4.500E+1	
H	κ^*	μ^*	6.000E+0	4.500E+1	
	p [MPa]	κ [MPa]	μ [MPa]	r_1 [MPa]	r_2 [−]
$\overline{R}$	1.000E+0	κ^*	μ^*	1.539E+3	1.583E+0
R	1.000E+0	κ^*	μ^*	1.539E+3	1.583E+0

The reference bulk and shear moduli are given by $\kappa^* = 2.200$E+3 [MPa] and $\mu^* = 5.000$E−1 [MPa].

acterized by contractions in the lateral directions. In order to obtain a relationship between the time rates of change of the axial stress and the lateral stretches we calculate the time rate of change of the Cauchy stress:

$$\dot{\boldsymbol{\sigma}} = -\frac{\dot{J}}{J}\boldsymbol{\sigma} + \mathbf{l}\boldsymbol{\sigma} + \boldsymbol{\sigma}\mathbf{l}^{\mathrm{T}} + \mathbb{c} : \mathbf{l}, \tag{15}$$

where $\mathbf{l} = \dot{\mathbf{F}}\mathbf{F}^{-1}$ is the spatial velocity gradient. In the case of uniaxial tension it can be shown that the kinematic quantities $\dot{J}/J$ and $\mathbf{l}$ are linear functions of the time rates of change of the logarithmic stretch rates $\dot{\overline{\ln[\lambda_\gamma]}}$, where λ_γ, $\gamma = 1, 2, 3$, are the principal stretches. For all deformations the lateral faces are traction free and we can write for the axial and lateral components of the normal stresses:

$$\begin{bmatrix} \dot{\sigma}_{11} \\ 0 \end{bmatrix} = \underbrace{\begin{bmatrix} c_{1111} + \sigma_{11} & 2(c_{1122} - \sigma_{11}) \\ c_{1122} & c_{2222} + c_{2233} \end{bmatrix}}_{\mathbf{e}} \begin{bmatrix} \dot{\overline{\ln[\lambda_1]}} \\ \dot{\overline{\ln[\lambda_2]}} \end{bmatrix}. \tag{16}$$

σ_{ij} and c_{ijkl} are the components of the Cauchy stress and the spatial stiffness, respectively.

The rates of the logarithmic stretch in axial and lateral directions can now be expressed as functions of the stress rate in the axial direction:

$$\dot{\overline{\ln[\lambda_1]}} = \frac{c_{2222} + c_{2233}}{\det[\mathbf{e}]}\dot{\sigma}_{11} \tag{17a}$$

$$\dot{\overline{\ln[\lambda_2]}} = -\frac{c_{1122}}{\det[\mathbf{e}]}\dot{\sigma}_{11}. \tag{17b}$$

For the case of an uniaxial tension on a linear elastic material, the Poisson's ratio ν can be obtained by $-\dot{\varepsilon}_2/\dot{\varepsilon}_1$. In analogy hereto an instantaneous Poisson's ratio ν_{inst} can be obtained in the case of finite deformations:

$$\nu_{inst} := -\frac{\dot{\overline{\ln[\lambda_2]}}}{\dot{\overline{\ln[\lambda_1]}}} = -\frac{\lambda_1}{\lambda_2}\frac{\dot{\lambda}_2}{\dot{\lambda}_1} = \frac{c_{1122}}{c_{2222} + c_{2233}}. \tag{18}$$

Bahuaud and Boivin (1968) presented the definition of an "actual" Poisson's coefficient ("coefficient de Poisson actuel") that corresponds to Eq. $(18)_2$ of our definition of the instantaneous Poisson's ratio. In contrast to the definition of a secant Poisson's ($\nu = -(\lambda_2 - 1)/(\lambda_1 - 1)$) Eq. (18) defines a tangent Poisson's ratio that is sensitive to the *rate of change of the volume*.

2.4. Condition number

A condition number c can be defined (see, e.g., Nipp and Stoffer, 1998) as the ratio of the maximum and the minimum eigenvalue of the spatial stiffness $\mathbb{c}$:

$$c := \frac{\max[\mathrm{eig}[\mathbb{c}]]}{\min[\mathrm{eig}[\mathbb{c}]]}. \tag{19}$$

A low condition number is favorable in computations.

3. Results

Simulations of the numerical example (cf. Section 2.2), using the quasi-incompressible formulations of the constitutive equations, reveal that only the models W, H and R reproduce the high stresses they showed while using the assumption of full incompressibility (cf. Fig. 2). The model $\overline{R}$ shows a slightly softer behavior while the two remaining models $\overline{W}$ and $\overline{H}$ are significantly too soft.

This goes in hand with the observation that the three models using the modified measures of the fiber stretch $\bar{I}_4$ and $\bar{\zeta}$, respectively, already violate the incompressibility constraint at rather small stretches (cf. Fig. 3).

An alternative and instructive representation of this effect is given in Fig. 4. For the models $\overline{W}$ and $\overline{H}$ the instantaneous Poisson's ratio ν_{inst} (cf. Eq. (18)) decreases, after being constant in the beginning, and even becomes negative at a critical stretch λ_{crit}, such that with increasing axial stretch the lateral stretch grows as well. Model $\overline{R}$ does not keep the Poisson's ratio constant equal 0.5 [−] either but shows a smaller deviation. The models W, H and R keep an instantaneous Poisson's ratio (close to) equal 0.5 [−], which agrees well with an (quasi) incompressible material.

Fig. 5 shows the condition number (cf. Eq. (19)) of all models. The models $\overline{W}$ and $\overline{H}$ have an only slightly increasing condition number until a critical stretch where the condition number begins to increase rapidly (in Fig. 5 the critical stretch λ_{crit} is shown for $\overline{W}$). This critical stretch is exactly at the value for which the instantaneous Poisson's ratio ν_{inst} passes through zero ($c_{1122} = 0$ [MPa], cf. Fig. 4). An analysis of the eigenvectors of the spatial stiffness tensor $\mathbb{c}$ reveals that for $\lambda_1 > \lambda_{crit}$, the deformation with the largest increase in the deformation energy is no longer volume change but rather axial stretch in the fiber direction.

The condition numbers for the models W and H (using I_4) are increasing much more than all other formulations and are, at $\lambda_1 = 1.2$ [−], two orders of magnitude higher than initially.

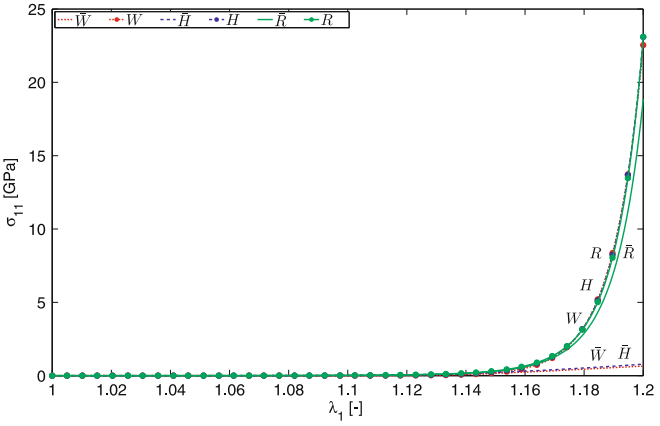

Fig. 2. Cauchy-stress σ_{11} in axial direction plotted against the axial stretch λ_1. The models $\overline{W}$ and $\overline{H}$ do not reproduce the high stresses observed while using the assumption of incompressibility during the parameter calibration; the model $\overline{R}$ behaves slightly softer.

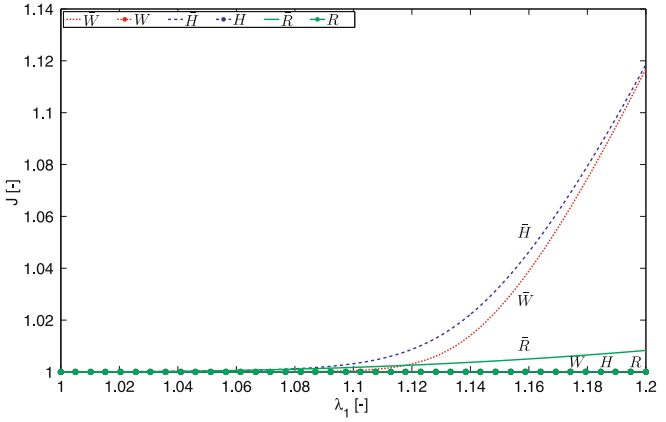

Fig. 3. Volume ratio J plotted against the axial stretch λ_1. Models W, H and R preserve the volume. The largest deviations from $J = 1$ [−] are obtained by the models $\overline{W}$ and $\overline{H}$.

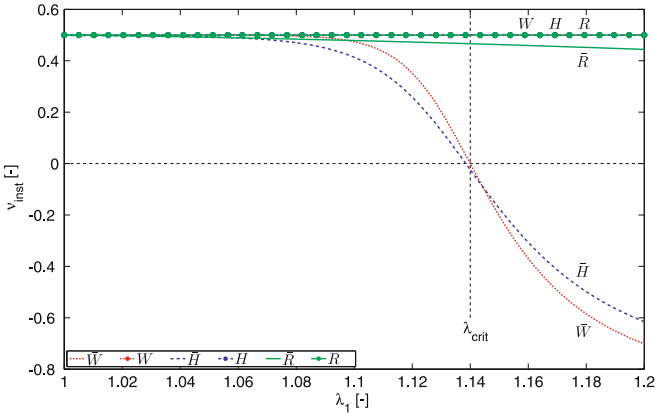

Fig. 4. Instantaneous Poisson's ratio ν_{inst} (cf. Eq. (18)) plotted against the axial stretch λ_1. For models $\overline{W}$ and $\overline{H}$ the ratio decreases to negative values indicating growing lateral stretches.

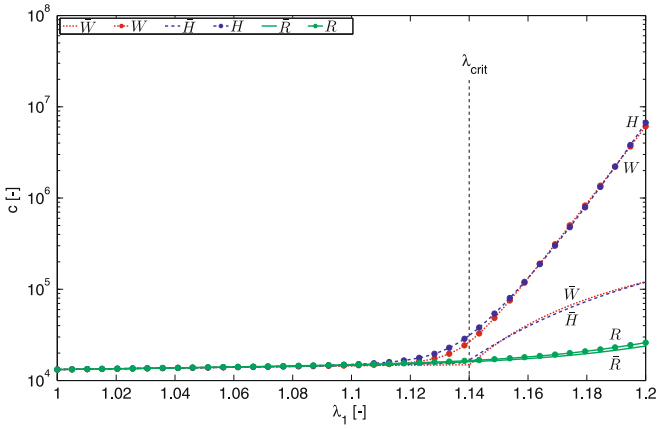

Fig. 5. Condition number c (cf. Eq. (19)) plotted against the axial stretch λ_1. Up to the critical stretch λ_{crit} (shown for $\overline{W}$) the condition numbers of models $\overline{W}$ and $\overline{H}$ increase only slightly, while the condition numbers for models W and H increase rapidly.

Both models $\overline{R}$ and R show only slightly increasing condition numbers.

4. Discussion

Our calculations show that for the quasi-incompressible formulation of the models $\overline{W}$, $\overline{H}$ and $\overline{R}$ the volume ratio J does not stay constant a priori (cf. Fig. 3). The first two models have in common that the deviatoric contribution of the ground substance and the volumetric contribution have polynomial forms while the fiber contributions are of exponential type. The latter model has a polynomial log-energy contribution of the fibers. This means that the fiber contributions $\overline{\Psi}_f$ and $\widehat{\Psi}_3$, respectively, grow much faster than the ground substance and volumetric contributions as their respective arguments increase.

The arguments of $\overline{\Psi}_f$ and $\widehat{\Psi}_3$, i.e., $\bar{I}_4$ and $\bar{\zeta}$, respectively, decrease with an increasing volumetric deformation (cf. Eq. (7)). Since the axial stretch is given by boundary conditions, the strain energy might be lowered through lateral expansion leading to an increasing volume ratio J and to a reduction in stress when compared to the incompressible case (cf. Fig. 2). Thus, the material tends, under uniaxial load, to a purely volumetric deformation state in order to lower the fiber energy at the expense of an increase in the ground substance and volumetric energy. The level of deformation at which this effect will take place depends on the specific formulation and the material parameters, in particular on the selected value of bulk modulus.

In Section 2.3, we showed that, in analogy to linear elasticity, we can define an instantaneous Poisson's ratio (18). This Poisson's ratio needs to be (close to) 0.5 [−] in order to describe an (nearly) incompressible material. For both models $\overline{W}$ and $\overline{H}$ the instantaneous Poisson's ratio deviates from the incompressible limit and becomes negative (cf. Fig. 4) even at seemingly innocuous strain levels. While the instantaneous Poisson's ratio of $\overline{R}$ departs as well from 0.5 [−] it does not do so as much as the other two models using the modified invariant $\bar{I}_4$.

The model proposed by Rubin and Bodner (2002) seems to be less sensitive to a use of the modified invariant $\bar{\zeta}$. The reason for this might be the fact that all contributions to the strain energy are in the exponent and are therefore more equilibrated in their contribution to the overall strain energy.

Changing the argument of the fiber contribution to I_4 disables the ability of the material to reduce its total energy by a more spherical deformation, due to the changed energetic couplings. Simulations indicate that with this change the volume ratio stays constant, equal to unity, and the instantaneous Poisson's ratio is kept close to 0.5 [−].

The unphysical response of growing lateral stretches in uniaxial tension has previously been reported in a different context by Ehlers and Eipper (1998). Their setting differs in two major points from ours: (1) they study isotropic materials and (2) in contrast to our assumption of (near) incompressible materials, they consider compressible materials with $\kappa/\mu = 5/3$ [−]. Ehlers and Eipper (1998) report growing lateral stretches when using strain energy forms that use an additive split into deviatoric and volumetric part equivalent to Eq. (8) without a fiber contribution. For axial stretches of up to $\lambda_1 = 10$ [−] none of the three models W, H and R of our study shows a growing lateral stretch when used without fibers ($w_3 = 0$ [MPa], $h_1 = 0$ [MPa] and $r_1 = 0$ [MPa], respectively). This was to be expected since we use a ratio κ/μ as high as 4400 [MPa]. The unphysical response reported in this paper originates from the fiber-reinforcement and is distinct from that studied by Ehlers and Eipper (1998). The underlying mechanism leading to this behavior, however, is the same: the total energy of the system can be lowered with a more spherical deformation in case of a large tangent stiffness related to the deviatoric energy contribution.

The models using $\bar{I}_4$ and $\bar{\zeta}$ can reduce the fiber contribution to the stiffness by volume growth and thus keep the condition number "moderate" (cf. Fig. 5). Using I_4 instead, the fibers contribute according to their true stretch and generate large entries in the stiffness matrix, thus leading to a dramatic enhancement of the condition number. This is not the case for the model proposed by Rubin and Bodner (2002), where an additive split is applied to the log-energies (cf. Eq. (11)); this formulation keeps the individual contributions closer together. The price for this is a more involved physical interpretation of each single term in the energy function as compared with the formulations using the additive split of the single contributions of spherical and distortional deformation of the isotropic ground substance and fiber stretch.

It has to be mentioned that if the true nature of a material is such that it combines fibers of exponentially increasing stiffness with a soft matrix the increase of the condition number corresponds to the physical reality and is therefore not bad or wrong a priori. Its negative implications for numerics have to be solved on the computational side.

The choice of the argument of $\overline{\Psi}_f$ also has consequences for the contributions of the fibers to the stress and stiffness. The Cauchy stresses due to the fibers can be written as

$$\bar{\boldsymbol{\sigma}}_f \sim \mathbf{F}\frac{\partial \bar{I}_4}{\partial \mathbf{C}}\mathbf{F}^{\mathrm{T}} = J^{-2/3}\mathbf{a} - \frac{1}{3}\bar{I}_4\mathbf{I} \tag{20a}$$

$$\boldsymbol{\sigma}_f \sim \mathbf{F}\frac{\partial I_4}{\partial \mathbf{C}}\mathbf{F}^{\mathrm{T}} = \mathbf{a}, \tag{20b}$$

where $\mathbf{a}$ is the structural tensor in the actual, deformed, configuration. It can clearly be seen that the use of I_4 leads only to stresses

along the fibers while using $\bar{I}_4$ induces stresses with components perpendicular to the fiber direction. The latter does not correspond to the idea of fibers behaving like uniaxial springs where (1) the resistance only depends on the stretch and (2) the corresponding force is in the direction of the spring. Also in the stiffness terms the use of $\bar{I}_4$ induces fiber contributions that are orthogonal to the fiber direction.

A more detailed discussion about the implications of either using $\bar{I}_4$ or I_4 on the coupling between deviatoric and spherical parts of deformation and stress can be found in Sansour (2008).

5. Conclusion

For isotropic materials the strain energy function is typically assumed to be a sum of purely deviatoric and purely spherical parts. This split was introduced and is used for its conceptual and numerical advantages, though Ehlers and Eipper (1998) showed that it can end in unphysical behavior if applied to materials not restricted to (near) incompressibility.

Later the idea of the additive split was extended to the case of anisotropic fiber-reinforced (nearly) incompressible materials, where the contributions of the matrix and the fibers were made dependent only on the deviatoric deformations. It was shown in this study that this approach might lead to undesired material responses, even for constitutive equations that meet the requirements of polyconvexity, and does violate the basic simplifying idea that fibers act as one-dimensional springs. For deformation states where the fiber contribution to the total deformation energy overwhelms the others, the material tends to reduce the fiber contribution through increasing spherical deformations. In the case of uniaxial tension this leads to undesired volume growth.

This effect can be avoided by introducing specific constraints in the numerical scheme such as Augmented Lagrangians, which effectively entails a change in the actual model to a strictly incompressible one. An alternative approach, suggested in this paper and which preserves the near incompressible character of the material, is to use I_4 in place of $\bar{I}_4$ for the fiber contribution to the strain energy function.

Weakening the principle of the additive split and allowing the fibers to contribute according to the total deformation solves the problem on a constitutive level. The fibers "feel" their true stretch and have therefore higher energy contributions than for the case with only deviatoric stretches. For models that use energy contributions of different orders of magnitude this results in a loss of accuracy for numerical schemes, shown by a strong increase of the condition number. This issue, however, is independent of the issue of constructing a proper model and its negative implications for numerics have to be solved on the computational side. For the case of uniaxial tension investigated in this work, the model presented by Rubin and Bodner (2002), which has more homogeneous fiber and matrix contributions, was shown to be more robust.

Acknowledgement

This work has been supported by the CO-ME/NCCR research network of the Swiss National Science Foundation (http://co-me.ch).

References

Antman, S.S., 2005. Nonlinear Problems of Elasticity. Springer, New York.
Bahuaud, J., Boivin, M., 1968. Étude du coefficient de Poisson pour des déformations élastiques, élastico-plastiques, petites ou finies. J. Mécanique 7, 141–153.
Balzani, D., Neff, P., Schröder, J., Holzapfel, G.A., 2006. A polyconvex framework for soft biological tissues. Adjustment to experimental data. Int. J. Solids Struct. 43, 6052–6070.
Eberlein, R., Holzapfel, G.A., Schultze-Bauer, C.A., 2001. An anisotropic model for annulus tissue and enhanced finite element analyses of intact lumbar disc bodies. Comput. Methods Biomech. Biomed. Eng. 4, 209–229.
Ehlers, W., Eipper, G., 1998. The simple tension problem at large volumetric strains computed from finite hyperelastic material laws. Acta Mech. 130, 17–27.
Flory, P.J., 1961. Thermodynamic relations for high elastic materials. Trans. Faraday Soc. 57, 829–838.
Hartmann, S., Neff, P., 2003. Polyconvexity of generalized polynomial-type hyperelastic strain energy functions for near incompressibility. Int. J. Solids Struct. 40, 2767–2791.
Holzapfel, G., 2000. Nonlinear Solid Mechanics a Continuum Approach for Engineering. Wiley, Chichester.
Holzapfel, G.A., Gasser, T.C., Ogden, R.W., 2000. A new constitutive framework for arterial wall mechanics and a comparative study of material models. J. Elasticity 61, 1–48.
Holzapfel, G.A., Gasser, T.C., Ogden, R.W., 2004. Comparison of a multi-layer structural model for arterial walls with a Fung-type model, and issues of material stability. J. Biomech. Eng. 126, 264–275.
MATLAB, 2005. The MathWorks, Inc., R14, Natick, MA 01760-2098, USA.
Nipp, K., Stoffer, D., 1998. Lineare Algebra. Eine Einführung für Ingenieure unter besonderer Berücksichtigung numerischer Aspekte. vdf Hochschulverlag, Zurich.
Ogden, R.W., 1972. Large deformation isotropic elasticity – on the correlation of theory and experiment for incompressible rubberlike solids. Proc. R. Soc. Lond. A Math. Phys. Sci. 326, 565–584.
Rivlin, R.S., Saunders, D.W., 1951. Large elastic deformations of isotropic materials. VII: Experiments on the deformation of rubber. Proc. R. Soc. Lond. A Math. Phys. Sci. 243, 251–288.
Rubin, M.B., Bodner, S.R., 2002. A three-dimensional nonlinear model for dissipative response of soft tissue. Int. J. Solids Struct. 39, 5081–5099.
Sansour, C., 2008. On the physical assumptions underlying the volumetric-isochoric split and the case of anisotropy. Eur. J. Mech. A Solids 27, 28–39.
Schröder, J., Neff, P., 2003. Invariant formulation of hyperelastic transverse isotropy based on polyconvex free energy functions. Int. J. Solids Struct. 40, 401–445.
Schröder, J., Neff, P., Balzani, D., 2005. A variational approach for materially stable anisotropic hyperelasticity. Int. J. Solids Struct. 42, 4352–4371.
Simo, J.C., Taylor, R.L., 1991. Quasi-incompressible finite elasticity in principal stretches. Continuum basis and numerical algorithms. Comput. Methods Appl. Mech. Eng. 85, 273–310.
Weiss, J.A., Maker, B.N., Govindjee, S., 1996. Finite element implementation of incompressible, transversely isotropic hyperelasticity. Comput. Methods Appl. Mech. Eng. 135, 107–128.